Outlier Removal in MEG Data for Imagined Speech Classification

Koki Nose*, Hajime Yano*, Tetsuya Takiguchi*, and Seiji Nakagawa†
* Graduate School of System Informatics, Kobe University, Kobe, Japan
E-mail: 250x055x@stu.kobe-u.ac.jp, hyano@port.kobe-u.ac.jp, takigu@kobe-u.ac.jp
† Center for Frontier Medical Engineering, Chiba University, Chiba, Japan
E-mail: s-nakagawa@chiba-u.jp

***Abstract*—This paper proposed an outlier removal method for magnetoencephalography (MEG) data during auditory imagery tasks to improve classification accuracy. While previous studies on imagined speech brain–computer interfaces (BCIs) mainly relied on electroencephalography (EEG), MEG offered higher spatial resolution but suffered from smaller data sizes, making it more sensitive to abnormal trials. To address outlier removal, we first pretrained a feature extractor on MEG data that had been augmented based on current source estimation. Second, we applied the trained feature extractor to obtain feature representations of the MEG samples. Third, these features were projected into a low-dimensional space using t-SNE. Outliers were then identified based on their deviation from the feature distribution and were removed before classifier retraining. Experimental results demonstrate that the proposed method improved classification accuracy, particularly when applied to both training and validation data. Furthermore, training the feature extractor on data augmented based on current source estimation likely led to clearer class boundaries, which further contributed to the performance improvement. These findings suggest that data augmentation based on current source estimation and t-SNE-based outlier detection enhance the robustness of MEG-based imagined speech decoding.**

I. Introduction

Brain–computer interfaces (BCIs) offer a vital communication and control channel for individuals with severe motor impairments. Among various BCI paradigms, those based on imagined speech have gained attention for their potential to enable intuitive and flexible control. While many studies utilize electroencephalography (EEG) [1]–[4], this work focuses on magnetoencephalography (MEG), a non-invasive neuroimaging technique with distinct advantages for this task [5].

MEG and EEG both offer excellent temporal resolution by directly measuring neural electromagnetic fields, but MEG provides better spatial resolution due to less signal distortion [6]. Compared to fMRI, which has superior spatial but poor temporal resolution from measuring blood-flow changes, MEG offers a compelling balance for decoding the rapid dynamics of imagined speech. However, the amount of MEG data that can be collected is often limited, as the required equipment is large-scale and less accessible than that for EEG.

Unlike image or audio data, anomalies in brain activity data—particularly during imagined speech—are difficult to verify, as it is not possible to confirm whether subjects truly imagined target words. One approach is to use dimensionality reduction to project signals into a low-dimensional space and identify significantly deviated samples as outliers. Such outlier detection techniques can automatically detect and remove anomalous trials, thereby improving the reliability of the training data and ultimately enhancing classification accuracy [7]–[9].

In this study, we aimed to improve the classification performance by removing outliers and pretraining the classifiers on the cleaned dataset. We projected the MEG signals into a low-dimensional space using dimensionality reduction techniques. Outliers were then identified based on their distance from the overall feature distribution and removed prior to classifier retraining. We also employed cortical source estimates obtained through source localization to generate augmented MEG data. These augmented data were then used to train a feature extractor that projects MEG signals into a low-dimensional space using t-SNE. This enhanced feature representation contributed to more robust outlier detection and ultimately led to improved classification performance in imagined speech decoding.

II. MEG Data

We used speech sound imagery MEG data measured by Uzawa *et al.* [5]. These data consist of MEG recordings from eight subjects (seven males and one female, aged 20–40 years old; mean ± SD: 24.3 ± 6.4 years). Although one subject (age 40) was notably older than the others (ages 20–23), the results for the oldest subjects were comparable to the results for the others in this study, suggesting that age was not a primary factor influencing the results. Necessary information regarding the experiment was given to the subjects, and informed consent was obtained prior to the experiment. The experiment was approved by the Institutional Review Board on Ergonomic Research of AIST. In each trial during the MEG measurements, the subjects listened to a speech sound twice and then imagined the speech sound as they listened to it, without

979-8-3315-7206-8/25/$31.00

moving their tongue and mouth. Three speech sounds of three Japanese words—"*amagumo*" (rain cloud), "*ibento*" (event), and "*uranai*" (fortune-telling)—were used. These words were selected because they are all common nouns with four morae, ensuring phonological consistency and high familiarity for the subjects. The duration of the speech sounds was 800 ms. The time intervals between the listening and the imagery in each trial were 500 ms. Three kinds of trials corresponding to the three words were conducted repeatedly and randomly. The number of trials for each word and for each subject was at least 100. MEG signals during the trials were measured using a 122-channel whole-head neuromagnetometer (Neuromag-122™, Neuromag, Ltd., Helsinki, Finland) with a sampling frequency of 400 Hz.

The measured MEG signals were downsampled to a sampling frequency of 200 Hz and digitally filtered to remove low-frequency components below 1 Hz. Signals from abnormal MEG sensors were removed and spatially interpolated based on signals from the other normal sensors. −100–900 ms signals after the start of the first listening and the imagery were extracted as MEG epochs during speech listening and imagery, respectively. MEG epochs that included signals with the peak-to-peak amplitude above 1000 fT/cm were removed. Ocular activities were also removed from the MEG signals using independent component analysis. This preprocessing was performed using MNE-Python [10].

III. Data Augmentation Based on Source Estimation

A. Formulation of Current Source Estimation

Finding the magnetic field observed by sensors when current sources in the brain are given is called a "forward problem". In this study, the brain region is discretized into a set of mesh points. The magnetic field $\boldsymbol{b}(t) \in \mathbb{R}^N$ observed by N sensors at time t is linearly related to the current vector $\boldsymbol{j}(t) \in \mathbb{R}^{3M}$ on M mesh points via a lead field matrix $\boldsymbol{L}$. The time-varying current vector $\boldsymbol{j}(t)$ represents the strength and orientation of current dipoles in the brain, comprising three orthogonal components at all mesh points. The relationship between $\boldsymbol{b}(t)$ and $\boldsymbol{j}(t)$ is expressed as

$$\boldsymbol{b}(t) = \boldsymbol{L}\boldsymbol{j}(t). \tag{1}$$

The lead field matrix $\boldsymbol{L}$ is given by numerical calculation, such as the boundary element method, which is based on the position of the sensor, the position of the mesh point, and the conductivity in the brain.

The inverse of the forward problem is to find the current source in the brain from the observed magnetic field containing noise. This is commonly referred to as the "inverse problem". When the brain is discretized, the number of current sources becomes very large compared to the number of sensors. This makes it difficult to uniquely obtain the current source from the observed magnetic field. This is known as an ill-posed problem. Conventional methods, such as MNE and sLORETA [11], assume the multivariate normal distributions for the prior distributions of noise and current sources contained in the observed values, and minimize the sum of the error and the regularization term between the forward problem and the observed value $\boldsymbol{b}_{\text{obs}}(t)$. It gives us an estimation $\hat{\boldsymbol{j}}(t)$:

$$\hat{\boldsymbol{j}}(t) = \underset{\boldsymbol{j}(t)}{\operatorname{argmin}} \|\tilde{\boldsymbol{b}}_{\text{obs}}(t) - \tilde{\boldsymbol{L}}\boldsymbol{j}(t)\|_2^2 + \lambda \boldsymbol{j}(t)^{\mathrm{T}} \boldsymbol{S}^{-1} \boldsymbol{j}(t) \tag{2}$$

$$= \boldsymbol{L}^{\mathrm{T}}(\boldsymbol{L}\boldsymbol{L}^{\mathrm{T}} + \lambda^2 \boldsymbol{I})^{-1} \boldsymbol{b}_{obs}(t), \tag{3}$$

where $\boldsymbol{S}$ is the covariance matrix of the parameters of the current source. However, it is difficult to obtain the probability distribution of the actual current source, and an estimation based on a prior distribution that differs from the actual one may result in a large error.

B. Data Augmentation

We applied a data augmentation method based on current source estimation to the MEG data recorded during speech imagery. First, we estimated the current sources $\hat{\boldsymbol{j}}(t)$ from the original MEG data using (2). Then, data augmentation was applied to the estimated sources as described below. The augmented current sources $\hat{\boldsymbol{j}}^{\text{aug}}(t)$ were subsequently transformed back into MEG signals using (1), resulting in new MEG data samples. These augmented data were used for training a classifier for outlier detection.

The augmentation procedure was as follows. A common threshold was computed across all current sources, and any source with a maximum instantaneous amplitude below this threshold was set to zero. The threshold was defined as

$$threshold = p \cdot \max_{l,t} |\hat{\boldsymbol{j}}_l(t)|, \tag{4}$$

where p is a parameter in the range [0, 1]. Here, $\hat{\boldsymbol{j}}_l(t) \in \mathbb{R}^3$ denotes the time-varying vector of the l-th current source, which corresponds to the three orthogonal components at a single mesh point. The signal $\hat{\boldsymbol{j}}_l(t)$ after applying threshold dropout is computed as follows:

$$\hat{\boldsymbol{j}}_l^{\text{aug}}(t) = \begin{cases} \boldsymbol{0} & (\max_t |\hat{\boldsymbol{j}}_l(t)| < threshold) \\ \hat{\boldsymbol{j}}_l(t) & (\text{otherwise}) \end{cases}. \tag{5}$$

This method generates cleaner data by dropping out low amplitude noise.

IV. Outlier Detection and Removal

In this study, to detect and remove outliers from MEG data recorded during speech imagery, we introduced a sample selection method based on latent features extracted from an intermediate layer of a trained classifier. The feature vector $\boldsymbol{x}$, used for dimensionality reduction, was extracted from each MEG signal using a pre-trained EEGNet model with its final classification layer removed. The classifier was trained on a dataset augmented via transformations in source space.

A. EEGNet

EEGNet [12] is a light-weight CNN architecture for EEG classification that uses depthwise separable convolution layers instead of ordinary convolution layers. EEGNet shows competitive performance with ordinary CNNs when a small amount of training data is available. EEGNet consists of an ordinary convolution layer on the time axis, a depthwise convolution layer on the sensor axis, a separable convolution layer, and a fully connected (FC) layer. In this study, the architecture of EEGNet was modified to use two separable convolution layers.

B. Overview of t-SNE

T-distributed stochastic neighbor embedding (t-SNE) is a nonlinear dimensionality reduction technique that maps high-dimensional data into a low-dimensional space for visual analysis and cluster structure exploration [13].

First, the similarity between two data points $\mathbf{x}_i$ and $\mathbf{x}_j$ in the high-dimensional space is defined as a conditional probability:

$$p_{j|i} = \frac{\exp\left(-\|\mathbf{x}_i - \mathbf{x}_j\|^2 / 2\sigma_i^2\right)}{\sum_{k \neq i} \exp\left(-\|\mathbf{x}_i - \mathbf{x}_k\|^2 / 2\sigma_i^2\right)}, \tag{6}$$

where σ_i is the bandwidth of the Gaussian kernel centered at $\mathbf{x}_i$, determined based on a user-specified perplexity that controls the local neighborhood size. The joint probability pij is symmetrized as

$$p_{ij} = \frac{p_{j|i} + p_{i|j}}{2n}, \tag{7}$$

where n is the number of data points.

Next, the similarity between corresponding points $\mathbf{y}_i$ and $\mathbf{y}_j$ in the low-dimensional space is modeled using a Student' s t-distribution with one degree of freedom:

$$q_{ij} = \frac{(1 + \|\mathbf{y}_i - \mathbf{y}_j\|^2)^{-1}}{\sum_{k \neq l} (1 + \|\mathbf{y}_k - \mathbf{y}_l\|^2)^{-1}}. \tag{8}$$

t-SNE minimizes the Kullback–Leibler (KL) divergence between the high-dimensional joint distribution $P = p_{ij}$ and the low-dimensional distribution $Q = q_{ij}$ by optimizing the positions of the embedded points $\mathbf{y}_i$:

$$\mathcal{L}_{\text{t-SNE}} = \text{KL}(P||Q) = \sum_{i \neq j} p_{ij} \log \frac{p_{ij}}{q_{ij}}. \tag{9}$$

By preserving the local structure of the data, t-SNE effectively projects data into two or three dimensions in a way that highlights clusters and local density variations. This makes it particularly suitable for visual detection of outliers and the identification of abnormal trials.

C. Outlier Detection Using t-SNE

In this study, we introduced an outlier detection method based on the distribution of MEG trials in the low-dimensional space obtained by t-SNE. Specifically, we computed the centroid of each class in the t-SNE space, and detected outliers based on the distance from the centroid.

For a class C_k composed of samples $\{\mathbf{y}_i\}_{i \in C_k}$ in the t-SNE space, the class centroid $\boldsymbol{\mu}_k$ is defined as

$$\boldsymbol{\mu}_k = \frac{1}{|C_k|} \sum_{i \in C_k} \mathbf{y}_i. \tag{10}$$

The Euclidean distance between a sample $\mathbf{y}_i$ and the class centroid $\boldsymbol{\mu}_k$ is computed:

$$d_i^{(k)} = \|\mathbf{y}_i - \boldsymbol{\mu}_k\|_2. \tag{11}$$

We applied the following two criteria to detect outliers:

1) **Intra-class Distance Based Removal :** Within each class C_k, the top p% of samples with the largest distances $d_i^{(k)}$ from the centroid are regarded as outliers. In this study, we set $p = 5$.
2) **Inter-class Boundary Based Removal :** A sample $\mathbf{y}_i$ is regarded as an outlier if the centroid of another class C_j $(j \neq k)$ is closer than its own class centroid $\boldsymbol{\mu}_k$, i.e.,

$$\exists j \neq k \text{ such that } \|\mathbf{y}_i - \boldsymbol{\mu}_j\|_2 < \|\mathbf{y}_i - \boldsymbol{\mu}_k\|_2. \tag{12}$$

These methods enable the automatic identification of samples that significantly deviate from the class structure. By removing such outlier trials and retraining the classifier, we aim to suppress the influence of abnormal data and improve classification performance.

V. Evaluation Experiment

EEGNet models that classified the MEG during the speech imagery were trained for each subject. The trained models were evaluated using 10-fold cross-validation. Each split set of the cross-validation was composed of successive MEG epochs. The temporally first 80% and the remaining 20% of the MEG epochs not included in the evaluation set were used for training and validating the models, respectively. Key training hyperparameters for the model were as follows: the Adam optimizer (learning rate: 1×10^{-3}) with a cross-entropy loss function. The models were trained for a maximum of 200 training epochs with a batch size of 128, utilizing an early stopping patience of 10 epochs based on the validation loss. A dropout rate of 0.25 was also applied during training.

The macro F1 score was used as the evaluation index for the trained EEGNet. This index is the average of the F1 scores calculated for each class, i.e. macro F1 = $\frac{1}{K}\sum_{k=1}^{K} \text{F1}_k$. The F1 score for the class k is defined as $\text{F1}_k = \frac{2\text{TP}_k}{2\text{TP}_k + \text{FP}_k + \text{FN}_k}$ where TP_k, FP_k, and FN_k are the number of true positives, false positives, and false negatives for the class k, respectively. The chance level of macro F1

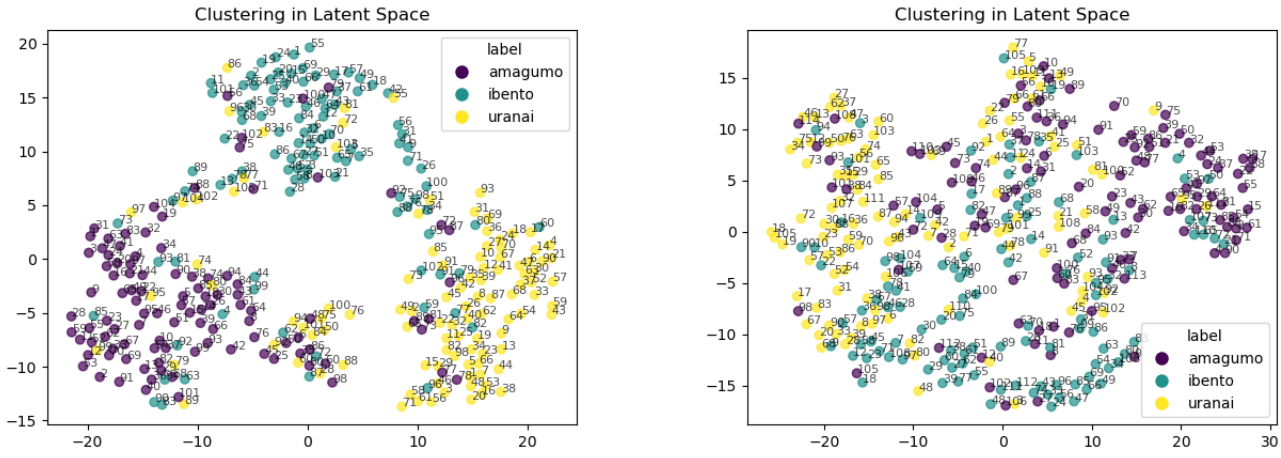

(a) Subject with well-separated classes

(b) Subject with overlapping classes

Fig. 1. Visualization of classwise embeddings in the t-SNE space

score for three-word classification is approximately 33%. The model with the maximum macro F1 score at the validation was selected and evaluated using the evaluation set.

VI. Results and Discussion

Examples of t-SNE visualizations of classwise embeddings are shown in Fig. 1(a) for the subject with the most clearly separated classes, and in Fig. 1(b) for the subject with the most overlapping ones. The degree of class separability varied across subjects, and in cases with substantial overlap, it became difficult to reliably identify outliers.

A. Intra-class Distance Based Removal

Table I shows the improvements in macro F1 scores obtained by applying intra-class distance-based outlier removal to speech imagery MEG data. In this method, data points located beyond a certain threshold distance from the class centroid are regarded as outliers and excluded from the dataset.

When outlier removal was applied only to the training data, the average improvement in macro F1 score was +1.3 points. This modest improvement suggests that eliminating noisy training samples slightly clarified the decision boundaries, leading to better classification performance. However, the effect was limited overall, and performance degradation was observed in some subjects. This implies that some of the removed samples, though identified as outliers, may have contained informative features relevant to classification.

When outlier removal was applied to both the training and validation data, the average improvement increased to +1.9 points. The removal of outliers from the validation set likely led to more accurate hyperparameter optimization, resulting in a more stable performance evaluation. Nonetheless, the improvements remained subject-dependent, with a few subjects showing reduced performance, again highlighting the sensitivity of the method to individual data characteristics.

TABLE I
Amount of the macro F1 score improvement using Intra-class distance based removal [%]

Removed set	**w/o aug.**	**with aug.**
w/o outlier removal	36.2 ± 4.5	
(1) Train	+1.1 ± 3.6	+1.3 ± 3.3
(2) Train + Valid	+1.3 ± 6.9	+1.9 ± 2.5
(3) Train + Valid + Test	+1.5 ± 3.7	+2.0 ± 3.8

Further, applying outlier removal to the test data resulted in the highest average improvement of +2.0 points among the three conditions. This result indicates that excluding anomalous samples from the evaluation set allows the classifier to be evaluated based on more representative data. However, modifying the test set should be seen as an upper bound on accuracy, not a realistic scenario.

In summary, while intra-class distance-based outlier removal contributed to improving classification performance by refining class structure in the embedded space, the effect was generally limited and varied across subjects. These results suggest that class separability and individual data distribution play a significant role in the effectiveness of outlier removal. For future work, it may be necessary to introduce adaptive thresholding strategies that consider the confidence level and density of each class to enhance robustness and reliability of anomaly detection.

B. Inter-class Boundary Based Removal

Table II shows the improvements in macro F1 scores when inter-class boundary-based outlier removal was applied to speech imagery MEG data, in comparison to models trained without any outlier removal. In this method,

TABLE II
AMOUNT OF MACRO F1 SCORE IMPROVEMENT BY COMBINING INTER-CLASS OUTLIER REMOVAL [%]

Removed set	**w/o aug.**	**with aug.**
w/o outlier removal	36.2 ± 4.5	
(1) Train	+1.5 ± 3.3	+2.6 ± 3.5
(2) Train + Valid	−0.7 ± 3.3	+2.8 ± 3.6
(3) Train + Valid + Test	+1.1 ± 2.7	+4.2 ± 8.3

samples in other class region are identified and removed as outliers. Table III shows the average percentage of samples identified as outliers for each subject, separately calculated for the Train, Validation, and Test phases. The high removal rate in validation and test sets occurred because the feature extractor, trained only on the training data, mapped these unseen signals to locations distant from the their class centroids.

TABLE III
AVERAGE PERCENTAGE OF OUTLIERS REMOVED PER SUBJECT IN EACH PHASE [%]

Subject	Train	Valid	Test
1	9.2	50.0	46.0
2	5.9	45.9	49.3
3	3.2	45.0	43.5
4	4.9	39.7	40.8
5	7.2	32.9	41.8
6	4.1	54.3	71.0
7	6.0	55.8	52.0
8	2.3	57.1	49.3

When outlier removal was applied only to the training data, a modest average improvement of +2.6 points in macro F1 score was observed. However, when the removal was applied to the validation or test data, the results exhibited greater inter-subject variability. For subjects who showed substantial improvement in classification performance, it is inferred that the removal procedure clarified the underlying class structure. Specifically, eliminating samples that overlapped with other class regions likely enhanced the separation between classes in the original high-dimensional space, thereby facilitating more accurate classification.

Conversely, for some subjects, a marked decrease in classification accuracy was observed. This may be due to the presence of highly overlapping classes prior to removal, where aggressive pruning distorted or destroyed the original class structure, leading to degraded performance.

These findings suggest that inter-class boundary-based removal is a potentially effective method for reinforcing class separability. However, its effectiveness is strongly dependent on the clarity of the initial class structure. Therefore, the degree of class separability should be assessed in advance to determine whether this method is appropriate for a given dataset.

A comparison between Tables II and III suggests a link between the number of outliers removed and classification performance. Subjects 3 and 4, who showed notable improvements in macro F1 scores, also had relatively high numbers of removed validation samples, indicating that eliminating overlapping samples can improve generalization. Conversely, Subject 6, with the highest removal counts in validation and test sets, exhibited less consistent improvement—possibly due to excessive pruning that disrupted the class structure. These findings imply that while moderate removal clarifies decision boundaries, overly aggressive exclusion may degrade performance.

TABLE IV
AMOUNT OF MACRO F1 SCORE IMPROVEMENT BY COMBINING INTER-CLASS AND INTRA-CLASS OUTLIER REMOVAL [%]

Removed set	**Mean ± std**
w/o outlier removal	36.2 ± 4.5
(1) Train	+2.8 ± 3.7
(2) Train + Valid	+1.4 ± 3.6
(3) Train + Valid + Test	+2.3 ± 6.9

C. Combined Outlier Removal: Intra- and Inter-class Integration

We also evaluated the effectiveness of combining intra-class and inter-class outlier removal methods. Table IV shows the improvements in macro F1 scores when both intra-class and inter-class boundary-based outlier removal methods were jointly applied to speech imagery MEG data, compared to models trained without any outlier removal.

When both intra-class and inter-class outlier removal methods were applied together, the resulting performance was comparable to that obtained using intra-class removal alone, but lower than the performance achieved with inter-class removal. This suggests that excessive sample removal during the combined outlier detection process may have led to overfitting. This over-removal likely resulted in overfitting to the remaining data, which may have contributed to the observed decrease in accuracy. These results highlight the importance of balancing the intensity of outlier removal with the preservation of data diversity. Maintaining this balance is crucial for ensuring robust model performance and generalization.

D. Effect of Data Augmentation on Outlier Detection

In both intra-class and inter-class outlier removal methods, we compared classification performance under conditions with and without data augmentation based on source estimation. Across all tested settings—regardless of whether outlier removal was applied to only the training set or both the validation and test sets—the models trained with data augmentation consistently achieved higher macro F1 scores (Tables I, II). This result highlights the significant contribution of data augmentation to overall classification performance.

A primary factor behind this improvement is the use of data augmentation in source space, which introduced physiologically meaningful variability into the training data. Unlike conventional signal-level perturbations, the augmentation applied to cortical current estimates preserved the spatial structure of neural activity, enabling

the model to capture more realistic neural dynamics. As a result, the feature extractor trained on this augmented data was able to learn a more structured and discriminative latent space, in which class representations appeared more clearly separated. This enhanced structural clarity facilitated more accurate detection of outliers based on class geometry.

Moreover, the augmented feature space appeared to yield more stable and well-defined decision boundaries, which is particularly beneficial for inter-class outlier removal methods that rely heavily on the separability of classes. The improved boundary clarity allowed for more precise exclusion of overlapping samples, thereby contributing to more effective classification.

These findings indicate that data augmentation serves not only to increase training set size, but also plays a critical role in shaping a more discriminative and robust feature space that benefits both classification and outlier detection. Thus, to fully leverage the potential of class-based outlier removal methods, it is essential to incorporate data augmentation during the training of the feature extractor.

VII. Conclusions

In this study, we investigated the effectiveness of outlier removal based on dimensionality reduction techniques for imagined speech classification using MEG data. By projecting the high-dimensional brain activity data onto a two-dimensional space and identifying and removing outliers, we observed improved classification accuracy in many subjects. Inter-class boundary based removal yielded better results than intra-class distance based removal, suggesting that eliminating samples overlapping with other regions is particularly beneficial. Furthermore, training feature extractors on source-space–augmented data likely enhanced class separability in the latent space, which contributed to more effective outlier detection and improved decoding performance. Consequently, outlier removal, especially when combined with data augmentation based on current source estimation, enables the training of more robust and reliable classification models for imagined speech decoding.

Acknowledgments

This work was supported in part by JSPS KAKENHI (Grant No. JP22K18423 and JP25K00660).

References

[1] C. H. Nguyen, G. K. Karavas, and P. Artemiadis, "Inferring imagined speech using EEG signals: A new approach using Riemannian manifold features," *J. Neural Eng.*, vol. 15, no. 1, 2017, Art. no. 016002.

[2] C. S. DaSalla, H. Kambara, M. Sato, and Y. Koike, "Single-trial classification of vowel speech imagery using common spatial patterns," *Neural Netw.*, vol. 22, no. 9, pp. 1334–1339, 2009.

[3] F. Li *et al.*, "Decoding imagined speech from EEG signals using hybrid-scale spatial-temporal dilated convolution network," *J. Neural Eng.*, vol. 18, no. 4, 2021, Art. no. 0460c4.

[4] A. Hernandez-Galvan, G. Ramirez-Alonso, and J. Ramirez-Quintana, "A prototypical network for few-shot recognition of speech imagery data," *Biomed. Signal Process. Control*, vol. 86, 2023, Art. no. 105154.

[5] S. Uzawa, T. Takiguchi, Y. Ariki, and S. Nakagawa, "Spatiotemporal properties of magnetic fields induced by auditory speech sound imagery and perception," in *IEEE Engineering in Medicine and Biology Conference (EMBC)*, 2017, pp. 2542–2545.

[6] M. Hämäläinen, R. Hari, R. J. Ilmoniemi, J. Knuutila, and O. V. Lounasmaa, "Magnetoencephalography—theory, instrumentation, and applications to noninvasive studies of the working human brain," *Rev. Mod. Phys.*, vol. 65, no. 2, pp. 413–497, 1993.

[7] J. Lin, Y. He, W. Xu, J. Guan, J. Zhang, and S. Zhou, "Latent feature reconstruction for unsupervised anomaly detection," *Applied Intelligence*, vol. 53, pp. 23 628–23 640, 2023.

[8] A. Dairi, N. Zerrouki, F. Harrou, and Y. Sun, "EEG-based mental tasks recognition via a deep learning-driven anomaly detector," *Diagnostics*, vol. 12, no. 12, 2022, Art. no. 2075–4418.

[9] O. E. Karpov *et al.*, "Evaluation of unsupervised anomaly detection techniques in labelling epileptic seizures on human EEG," *Appl. Sci.*, vol. 13, no. 9, 2023, Art. no. 2076–3417.

[10] A. Gramfort *et al.*, "MEG and EEG data analysis with MNE-Python," *Front. Neurosci.*, vol. 7, p. 267, 2013.

[11] R. D. Pascual-Marqui, "Standardized low-resolution brain electromagnetic tomography (sLORETA): Technical details," *Methods Find. Exp Clin. Pharmacol.*, vol. 24, no. D, pp. 5–12, 2002.

[12] V. J. Lawhern, A. J. Solon, N. R. Waytowich, S. M. Gordon, C. P. Hung, and B. J. Lance, "EEGNet: A compact convolutional neural network for EEG-based brain–computer interfaces," *J. Neural Eng.*, vol. 15, 2018, Art. no. 056013.

[13] L. van der Maaten and G. Hinton, "Visualizing data using t-SNE," *J. Mach. Learn. Res.*, vol. 9, pp. 2579–2605, 2008.